Thermal Science and Engineering Progress 5 (2018) 555–567

Contents lists available at ScienceDirect

Thermal Science and Engineering Progress

journal homepage: www.elsevier.com/locate/tsep

Dynamic simulation and parametric sensitivity study in reactive CO_2 capture systems – A solvent comparison study

L. Prentza*, I.P. Koronaki, E.G. Papoutsis, V.D. Papaefthimiou

Laboratory of Applied Thermodynamics, School of Mechanical Engineering, Thermal Engineering Section, National Technical University of Athens, Heroon Polytechniou 9, Zografou Campus, 15780 Athens, Greece

ARTICLE INFO

Keywords:
Dynamic model
Reactive absorption
CO_2
Alkanolamines
Parametric analysis
Sensitivity analysis
FDM

ABSTRACT

The control of CO_2 emissions released in the atmosphere is an indisputable need in order to avoid environmental and health consequences, as well as to reach European and global targets for climate change confrontation. During the last decades, various methods have been proposed towards this direction. As fossil fuels remain dominant in the energy field, technologies focused on CO_2 capture have been developed, known as Carbon Capture Systems (CCS). During the last decade, CCS have managed to become cost-competitive in relation to other technologies. However, CCS need to receive strong policy support in order to develop solid and applicable business cases. This work studies reactive absorption, a post-combustion method to remove CO_2 from flue gases using aqueous chemical solutions that react with CO_2 and capture it. In specific, this paper focuses on two alkanolamines as absorbents, Monoethanolamine (MEA) and 2-amino-2-methyl-1-propanol (AMP).

Following previous work, a dynamic model was developed in Matlab®, simulating transient behavior of a packed column for reactive absorption. The methodology followed to solve the set of partial differential equations describing the problem was the Finite Differences Method (FDM). Based on experimental data from a pilot plant various scenarios were tested in order to investigate the reaction of the system in different operational perturbations, such as flow disturbances, changes in temperature and in the solution's molarity. These factors were studied parametrically and the outcome of these simulations was used to perform a Sensitivity Analysis (SA) in order to determine the important parameters influencing CO_2 absorption performance.

The parametric analysis showed that the inlet gas flow rate was the most influential factor determining the CO_2 absorption level for both solvents. In following, the temperature of the liquid entering the column was also statistically important having strong impact on absorption. Surprisingly, the flow of the lean solvent wetting the column seems to have lower impact than the gas flow. Thus, increased solvent flow does not ensure respective enhancement of the CO_2 absorption. Molarity is also very important as the quantity of amine in the solution determines the quantity of the captured CO_2. In terms of reaction time towards disturbances, changes in liquid molar flow, liquid temperature and molarity seem to lead to higher reaction time until the system reaches a new steady state value (2–5 min). Finally, the results showed that there is a maximum capture level, beyond which the absorption cannot be further enhanced for specific conditions.

1. Introduction

Minimizing CO_2 emissions remains a challenge when dealing with the environmental footprint of various technologies and processes (fossil power plants, cement production units, vessels, other industrial processes, etc.). In 2014, fossil fuels continued to be the major contributor to net electricity production in the EU-28. Despite Renewable Energy Sources (RES) wide penetration in the electricity grid, combustible fuels are estimated to be nearly one half (49.8%) of total net electricity generated [14]. Different CO_2 capture techniques known as CCS (Carbon Capture Systems) have been proposed, taking place before or after fuel processing, thus categorized as pre/post combustion CO_2 capture respectively. Post-combustion capture is easier to implement as a retrofit option for existing plants because radical changes are not needed [25]. Both methods have similar considerable costs, e.g. burdening the levelised cost of electricity about 50%, for the case of coal/gas power plants [13]. This significant cost is expected to be diminished, via further enhancement and optimization of the process with measures proposed by various researchers. For example, measures targeting to the intensification of the process, such as usage of rotating

* Corresponding author.
E-mail addresses: prentzaloukia@central.ntua.gr (L. Prentza), koronaki@central.ntua.gr (I.P. Koronaki), sparou@central.ntua.gr (E.G. Papoutsis), vpapaeft@central.ntua.gr (V.D. Papaefthimiou).

https://doi.org/10.1016/j.tsep.2018.02.012
Received 25 October 2017; Received in revised form 16 February 2018; Accepted 17 February 2018

Nomenclature

Symbol	Parameter (Unit)
A	column cross-sectional area ($m^{2)}$
a_w	specific wetted area ($m^2/m^{3)}$
C_i^G	gas component molar concentration (mol/m^3)
C_i^L	liquid component molar concentration (mol/m^3)
$C_{L,MEA}^f$	liquid molar concentration of free MEA (mol/m^3)
$C_{L,AMP}^f$	liquid molar concentration of free AMP (mol/m^3)
$D_{L,CO2}$	CO_2 diffusivity in the amine solution (m^2/s)
ΔH_{CO2}	heat of CO_2-amine reaction (J/mol)
ΔH_{H2O}	heat of condensation (J/mol)
E	enhancement factor (−)
G	volumetric gas flow rate (m^3/s)
h_L	liquid holdup (−)
K_{Gi}	component overall mass transfer coefficient (mol/(m^2sPa))
k_{Gi}	component gas-side mass transfer coefficient (mol/(m^2sPa))
k_{Li}	component liquid-side mass transfer coefficient (m/s)
k_2	reaction rate constant (m^3/(mol s))
L	volumetric liquid flow rate (m^3/s)
M_i	component molecular mass (kg/mol)
N_i	interfacial component molar flux (mol/(m^2s))
p_i	partial pressure (Pa)
p_i	equilibrium partial pressure (Pa)
q	interfacial heat flux (J/(m^2s))
ρ_G	gas phase density (kg/$m^{3)}$
ρ_L	liquid phase density (kg/$m^{3)}$
T_G	gas phase temperature (K)
T_L	liquid phase temperature (K)
u_G	superficial gas velocity (m/s)
u_L	superficial liquid velocity (m/s)

beds, high concentration solvents, alternative solvents are proposed [26,28] with promising results. These techniques should firstly be studied in a theoretical level through research and simulations. Concluding, there is a need for thorough studies simulating the process dynamically in order to reach more satisfactory levels of system's overall efficiency.

The current work studies one of the most popular post-combustion methods, the chemical or reactive absorption. During reactive absorption both physical absorption and chemical reactions occur. The capture of free CO_2 by the absorbent bulk via chemical reactions permits further dissolution of the pollutant in the absorption mean, improving the system's efficiency. Solvent absorption ensures high capture efficiency and selectivity, and reduced capital and operating costs as well as enhanced energetics and possibility for modular approaches [9]. For CO_2 reactive absorption, aqueous solvents of alkanolamines are widely used, due to their strong reactivity with CO_2 molecules which make them suitable for low CO2 concentrations; existing coal power plants have a low concentration of CO_2 (13–15% wet basis) [24].

The process usually takes place in packed absorption beds/columns. The usually cylindrical column is filled with packing material (random or structured) and the two streams (flue gas and lean solvent) are flowing counter-currently interacting through mass and heat transfer. This process is usually simulated by the two-film mass transfer theory [29], schematically shown in Fig. 1. Molecular CO_2 is diffused through the gas film, is then absorbed in the liquid and subsequently diffuses through the liquid film.

Studying literature, various models can be found simulating the steady state phenomenon of reactive absorption in one or two spatial dimensions providing concentration and temperature profiles along the absorption column or across the column sectional area [2,7,1,22]. These models include both kinetic and thermodynamic aspects and aim to the optimization of the absorption process. It is recently though, that more of these attempts include dynamic characteristics and more realistic representations of the process [8,10,20,15,21]. On the other hand, dynamic simulation of the process is indispensable as the flue gas channeled in the column is often characterized by disturbances due to operational perturbations during combustion or other reasons. For example, power plants in UK may need to increase their output by 10% within only 10 s due to changes in real-time demand [21]. In case of biofuels and coal-based power plants, the condition of the fuel might vary during operation implying varying flue gas composition [4]. Such changes have a significant effect on the absorption efficiency of a CCS unit and their dynamic simulation is challenging including multiple factors hindering the mathematical modelling.

2. Mathematical model

The CO_2 absorption by alkanolamines is described by the following set of partial differential equations deriving by mass and heat balances, where index i characterizes the individual components of each phase:

$$h_L \frac{\partial L}{\partial t} = -\frac{\partial (u_L L)}{\partial z} + \frac{u_L A a_w}{\rho_L} \sum (M_i N_i) \tag{1}$$

$$(1-h_L)\frac{\partial G}{\partial t} = -\frac{\partial (u_G G)}{\partial z} - \frac{u_G A a_w}{\rho_G} \sum (M_i N_i) \tag{2}$$

$$h_L \frac{\partial C_i^L}{\partial t} = -\frac{\partial (u_L C_i^L)}{\partial z} - a_w N_i \tag{3}$$

$$(1-h_L)\frac{\partial C_i^G}{\partial t} = -\frac{\partial (u_G C_i^G)}{\partial z} + a_w N_i \tag{4}$$

$$h_L \frac{\partial T_L}{\partial t} = -\frac{\partial (u_L T_L)}{\partial z} + \frac{a_w}{\sum C_i^L C_{p,i}} (q + \Delta H_{CO2} N_{CO2} + \Delta H_{H2O} N_{H2O}) \tag{5}$$

$$(1-h_L)\frac{\partial T_G}{\partial t} = -\frac{\partial (u_G T_G)}{\partial z} - \frac{a_w q}{\sum C_i^G C_{p,i}} \tag{6}$$

Certain parameters of the aforementioned equations are explained below.

The interfacial molar flux of the volatile components is given by the following equation based on the two-film model:

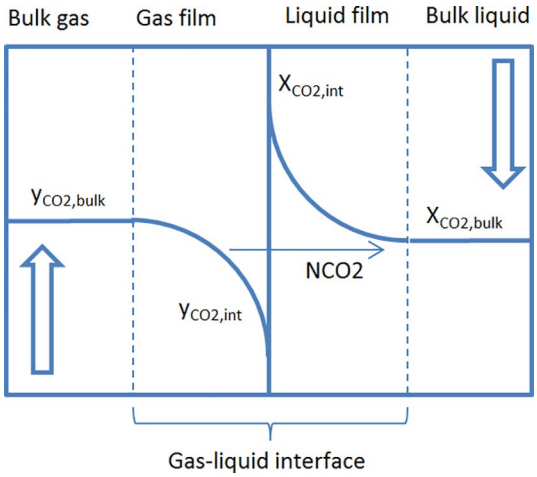

Fig. 1. Schematic illustration of the two-film theory on reactive absorption.

$$N_i = K_{Gi}(p_i - p_i) \quad (7)$$

where p_i is the partial pressure of the volatile components in the gas phase and p_i^* is the equilibrium partial pressure of these components, meaning the pressure that the component would have if it was in equilibrium with the liquid phase. Their difference expresses the *driving force* causing the absorption phenomenon. Theoretically, when they reach equal values, the absorption is terminated, as the solvent reaches saturation.

K_{Gi} is the overall mass transfer coefficient calculated for the volatile components as follows:

For CO_2 the overall K_{GCO2} is determined by the equation with two terms considering both gas side and liquid side resistance in mass transfer. The liquid side coefficient is corrected with the enhancement factor, taking into account the enhancement of the absorption due to chemical reaction.

$$\frac{1}{K_{GCO2}} = \frac{1}{k_{G,CO2}} + \frac{H_{CO2}}{Ek_{L,CO2}} \quad (8)$$

For water, it is assumed that the liquid-side mass-transfer resistance is negligible, thus the overall mass transfer coefficient is equal to the gas side mass transfer coefficient for water:

$$K_{GH2} = k_{G,H2O} \quad (9)$$

In the context of this work, amine is considered to be non-volatile, thus no flux is assumed to occur between the two phases (there is no amine in the gas phase).

The individual component mass transfer coefficients $k_{G,i}$ and $k_{L,i}$ and the specific wetted area a_w were determined by Billet and Schultes correlations [3]. u_G and u_L are the superficial velocities of the two countercurrent streams. The liquid hold-up of the column h_L was calculated by a Billet and Schultes correlation.

For AMP the enhancement factor was calculated by a correlation given by Danckwerts [5], assuming that the amine concentration is the same at the gas–liquid interface and at the liquid bulk:

$$E = \sqrt{1 + Ha^2} \quad (10)$$

Ha is Hatta number and is equal to:

$$Ha = \frac{\sqrt{k_2 C^f_{L,AMP} D_{L,CO2}}}{k_{L,CO2}} \quad (11)$$

where $C^f_{L,AMP}$ is the concentration of the free AMP in the liquid, given by a VLE model [7], $D_{L,CO2}$ is the diffusivity of CO_2 in the amine solution and k_2 is the second-order reaction rate constant.

For MEA the enhancement factor was determined by an explicit correlation given below [6]:

$$E = \frac{\sqrt{k_2 C^f_{L,MEA} D_{L,CO2}}}{k_{L,CO2}} \quad (12)$$

where $C^f_{L,MEA}$ is the concentration of the free MEA in the liquid, given by a VLE model [12], $D_{L,CO2}$ is the diffusivity of CO_2 in the amine solution and k_2 is the second-order reaction rate constant.

The second order reaction rates were given by Saha and al. [23] for AMP and by Hikita et al. [11] for MEA.

The interfacial heat flux between the gas and the liquid phase is determined by the following equation, where h is the heat transfer coefficient in the gas phase given by the Chilton–Colburn analogy correlation:

$$q = h(T_G - T_L) \quad (13)$$

Targeting to the simplicity of the model several assumptions were performed:

1. Amine is considered to be non-volatile
2. All reactions are considered to take place in the liquid film, while the liquid bulk is in equilibrium
3. The interface temperature is equal to the bulk temperature
4. The liquid-side mass-transfer resistance for the volatile solvent is negligible
5. The interfacial surface is the same for both heat and mass transfer
6. Axial dispersion is not considered
7. Adiabatic conditions for the absorption column
8. Liquid and gas phase are considered as ideal mixtures
9. Liquid holdup remains constant along the column

More information on the parameters of the model and the literature source of physical properties of the components are provided in previous work of the researchers [18].

3. Computational method

The problem of reactive absorption via countercurrent flow in an absorption column is mathematically modelled by a set of parabolic partial differential equations, framed by boundary conditions in two points, namely the two ends of the column. Various software packages are offered solving these types of problems (COMSOL, gPROMS, Aspen plus, etc.) used by many researchers [10,21,30]. Others researchers built ad hoc codes using various numerical or analytical methods in order to solve these equations. [10,8,15]. In this work, a code based on Finite Differences Method was developed in Matlab®, using the forward finite difference relation for the upstream gas flow PDEs and the backward finite difference method to discretize the equations referring to the downstream flow of the amine aqueous solution.

4. Model steady state validation

Steady state validation of the model outcomes has been performed against published experimental data from a pilot plant installed in the University of British Columbia in Canada [27] and was reported in detail in previous work [18]. Tontiwachwuthikul conducted experiments using monoethanolamine (MEA), 2-amino-2-methyl-1-propanol (AMP) and sodium hydroxide (NaOH) aqueous solvents. For the steady state validation, two run tests were used: T25 using AMP and T15 using MEA. The conditions of these tests are given briefly in Table 1. The pilot absorption column was made of acrylic plastic and had 0.1 m internal diameter, filled with 12.7 mm ceramic Berl saddles random packing. The column operated under atmospheric pressure and the total packing height was 6.55 m.

The solution of the steady state equations was obtained by setting the time derivatives in Eqs. (1)–(6) equal to zero and finally resulted to composition, flow and temperature profiles. The predictions were accurate, validating the efficiency of the model. The analytical profiles (CO_2 mole fraction, liquid temperature, rich loading) are not presented here for reasons of brevity but are thoroughly explained in previous work of the researchers [18].

5. Dynamic simulations

The dynamic simulations performed in this work examine two stages of the absorption process in order to study transient behavior.

Table 1
T25 (AMP) and T15 (MEA) inlet conditions.

Tontiwachwuthikul data	T25 (AMP solvent)	T15 (MEA solvent)
Liquid flow rate	9.5 m^3/m^2 h	13.5 m^3/m^2 h
Initial solvent concentration	2.00 kmol/m^3	2.03 kmol/m^3
Inlet liquid temperature	288 K	292 K
Initial liquid loading	0.152	0.0
Gas flow rate	14.8 mol/m^2 s	14.8 mol/m^2 s
Gas Composition	CO2: 18.9%	CO2: 19.5%

The first stage is the start-up process where the column is considered to be initially filled in only with the lean solvent, whereas the gas begins to flow gradually increasing its flow rate from zero to a constant desirable value (full load). The second stage includes different scenarios related with disturbances occurring in the middle of a steady state operation. The effect of altering inlet flue gas flow rate, inlet liquid flow rate, L/G ratio, gas and liquid inlet temperatures and initial amine molarity is investigated in time depth.

For the start-up scenario, the initial conditions are the constant values of the liquid characteristics, as the column is assumed to be only filled in with liquid; whereas the initial conditions for the gas equations were set equal to zero. For the disturbances considered to occur during steady state operation, the outcomes of steady state simulations (concentration, flow and temperature profiles along the column during steady state operation) were used as initial conditions. The boundary conditions are in both cases the inlet conditions of the two fluids as described in Tables 1 and 2, altering each time the factor to be studied.

These simulations were conducted for the two alkanolamine aqueous solvents mentioned before, MEA and AMP, in order to investigate any differences in the response of these absorbents to operation perturbations. MEA is a primary amine and thus is very reactive with CO_2. However, it requires high amounts of energy for regeneration and is characterized by mediocre capacity. AMP belongs to a different category of alkanolamine-based gas absorbents, the sterically hindered amines, and is the hindered form of MEA. AMP reacts with the rate of a primary amine and has the capacity of a tertiary amine.

5.1. AMP dynamic parametric simulations

As mentioned before, the column is assumed to be filled in with flowing lean liquid while the gas is gradually entering the column increasing its flow rate from zero until it reaches the final desirable flow of Table 1. The conditions of start-up process are shown in Table 2. Then, after a period of steady state operation with no changes occurring, the following scenarios were tested, shown in Table 3 having effect on the CO_2 absorption efficiency:

1. Inlet gas flow linearly increases/decreases 10 and 20%, keeping the liquid flow constant.
2. Inlet liquid flow linearly increases/decreases 10 and 20%, keeping the gas flow constant.
3. Inlet liquid and/or gas flows are altered, testing different values of L/G ratio.

a. Both L and G increase linearly keeping L/G ratio constant (same as steady state). Flows are increased up to 10% from their initial value.
b. Both L and G change linearly to a new constant L/G ratio (100% increase in relation to initial steady state). Both L and G are linearly increased.
c. Both L and G change linearly to a new constant L/G ratio (50% decrease in relation to initial steady state). G is linearly increased and L is linearly decreased.
d. G is kept constant with the same value as in steady state, while L is instantly increased so as the L/G ratio is doubled.
e. G is kept constant with the same value as in steady state, while L is instantly decreased so as the L/G ratio is reduced to half in comparison to the steady state operation ratio.

4. Inlet liquid temperature increases/decreases linearly up/down to various values.
5. Inlet gas temperature increases/decreases linearly up/down to various values.
6. Initial amine concentration is varied at one time step (not linearly) as a boundary condition of the problem.

Changes occurring linearly are assumed having a duration of 6 min and to be followed by a new steady state operation of additional 6 min, while scenarios 3 d,e,f and 6 are considered to happen instantly, while their progress is monitored for 6 min. Table 3 briefly presents the aforementioned dynamic scenarios and Figs. 2–11 illustrate these processes, presenting the CO_2 capture level profile during these changes.

5.1.1. Start-up

As seen in Fig. 2, during the first couple of minutes the absorption capacity of CO_2 reaches 100%. During the first seconds of the start-up process the gas is still filling the column, thus there is no CO_2 concentration at the upper part of the column and this leads to a fictitious absorption equal to 100%. Afterwards, this percentage is still the same as the quantity of CO_2 in the gas phase remains low and can be fully absorbed by the amine solvent. After 2 min, the absorption level decreases, as the inlet gas flow linearly increases from 0 m^3/sec to 0.0028 m^3/sec within an overall time interval of 6 min from the beginning of the process. When gas flow reaches the desirable level (full load) the absorption is taking place under steady state conditions. As seen in the diagram, there is no considerable reaction time as the absorption level is stabilized almost immediately after the establishment of steady state conditions. However, there is a very slight increase in the absorption level until minute 10, until it completely reaches the new steady state condition. As expected, the final absorption performance (56.7%) in steady state conditions has negligible deviation from the absorption level as calculated in steady state validation (57.7%).

In Fig. 3, the profiles of liquid temperature along the column are given for various moments during start-up and the steady state operation phase that follows. Observing the liquid temperature profile along the column, it is seen that the temperature reaches a highest value at a point near the bottom of the column and then drops significantly. This curve is called “temperature bulge” and has been observed in literature [e.g. [19]]. As seen in the diagram, the temperature bulge moves higher along the column in time depth. Studying the outcomes of various steady state models, it is observed that the CO_2 concentration is decreasing from the bottom to the top of the column, as it is captured by the amine. The rise of the liquid temperature is mainly due to the highly exothermic reaction occurring between CO_2 molecules and the amine. Thus, it was expected that the temperature bulge is placed closer to the bottom as there is more CO_2 to react and consequently higher heat of reaction is released. For the same reason, the liquid temperature reaches higher values as the gas flow rate increases in time. The drop of the liquid temperature at the bottom of the column is caused by the entrance of the gas in lower temperature. The increase of the gas flow causes also the relocation of the temperature bulge higher in the column as there is more CO_2 to react with the amine and the temperature reaches higher values; however more time is needed to achieve these temperatures moving the bulge higher in the column.

Another important parameter is rich loading, thus its evolution during start-up is presented in Fig. 4. As seen there is a response time of approximately 3 min from the steady state operation establishment (6 min) until rich loading reaches a new steady value.

5.1.2. Inlet gas flow parametric study

This section will examine the effect of inlet gas flow on the absorption performance dynamically. The gas flow is assumed to be linearly increased/decreased 10% and 20%. As expected, the absorption level decreases as the gas flow increase. This decrease is due to the fact that there is more CO_2 available to be captured by the amine, hindering the absorption. Respectively, the CO_2 capture is enhanced when gas

Table 2
Start-up scenario for AMP – T25.

Start-up scenario	Duration (min)	Inlet gas flow (m3/sec)	Inlet liquid flow (m3/sec)
	6	0–0.0028 (linearly increased)	0.0000207 (constant)

Table 3
Dynamic simulation scenarios for AMP – T25.

Phase I: Disturbance scenarios						
1	2		3	4	5	6
Gas flow parametric (m^3/sec)	Liquid flow parametric (m^3/sec)		L/G ratio parametric	Inlet liquid temperature parametric (K)	Inlet gas temperature parametric (K)	Amine initial concentration (mol/m^3)
G	L	G	L	L/G	TL (linearly up/down to)	TG (linearly up/down to)	C_{amine}
From 0.0028 to ± 10, 20% (linearly)	0.0000207 (constant)	0.0028 (constant)	From 0.0000207 to ± 10,20% (linearly)	a 0.00739 (same as steady state)	280	280	3000
				b 0.0147	284	284	4000
				c 0.0037	292	292	5000
				d 0.0147 (G constant)	296	296	
				e 0.0037 (G constant)	300	300	
Phase II: New steady state operation (Duration: 6 min) *Operating with the final conditions after the end of the disturbance*							

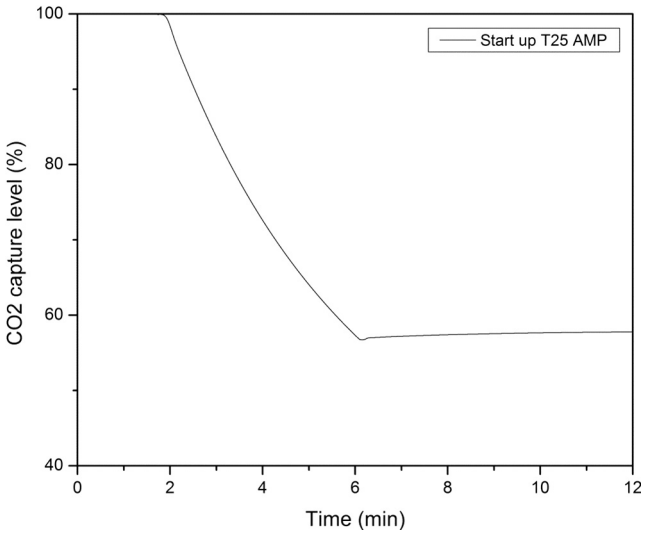

Fig. 2. Start up-T25 AMP.

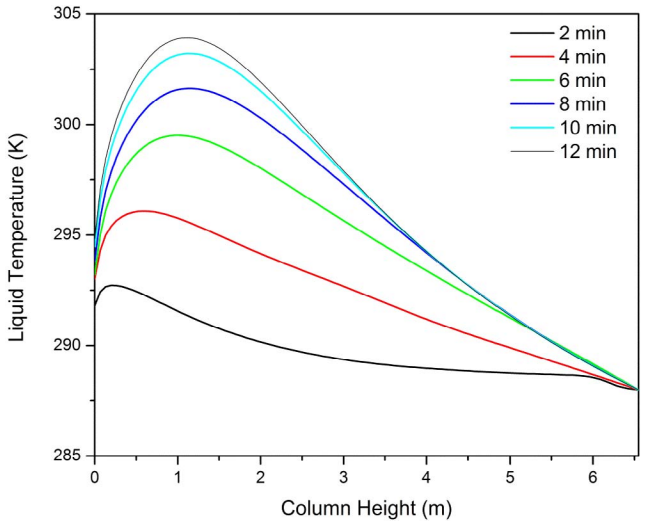

Fig. 3. Liquid Temperature profiles during start-up and steady state operation -AMP.

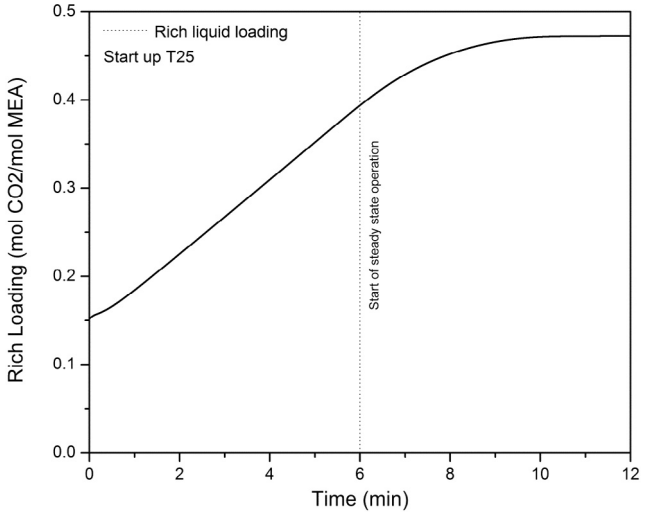

Fig. 4. Rich loading profile for start-up (T25-AMP).

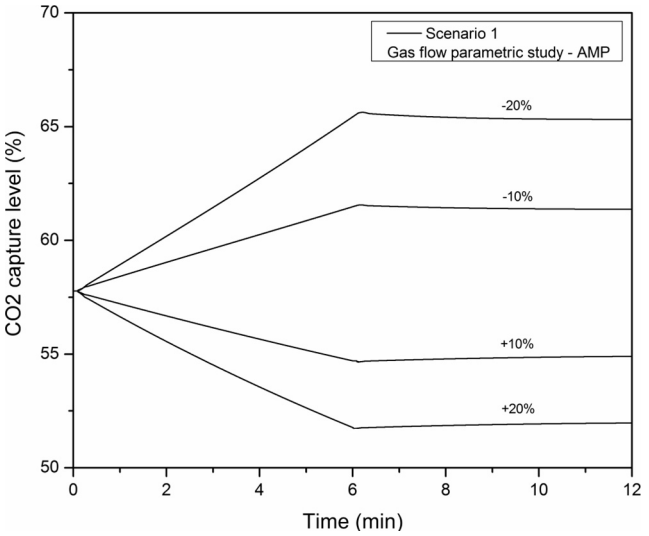

Fig. 5. Gas flow parametric study-AMP.

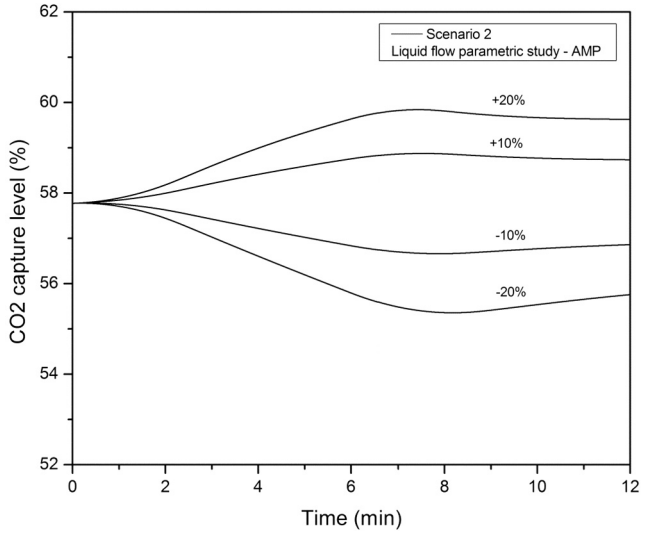

Fig. 6. Liquid flow parametric study-AMP.

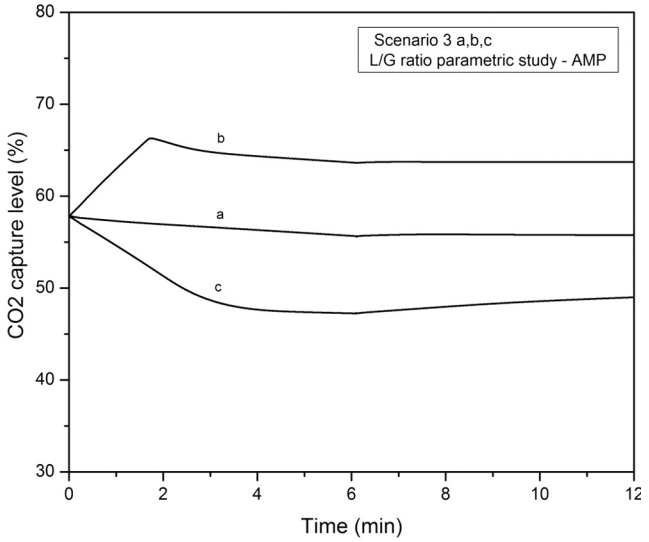

Fig. 7. Scenarios 3 a, b, c: L/G ratio parametric study-AMP.

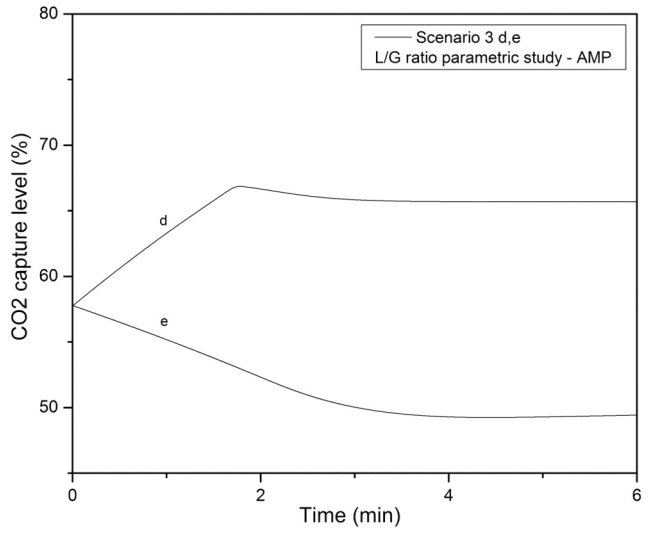

Fig. 8. Scenarios 3 d, e: L/G ratio parametric study-AMP.

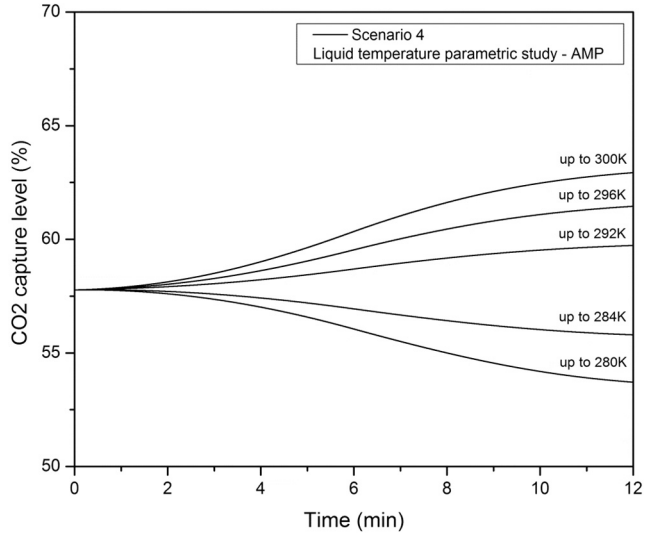

Fig. 9. Liquid Temperature parametric study-AMP.

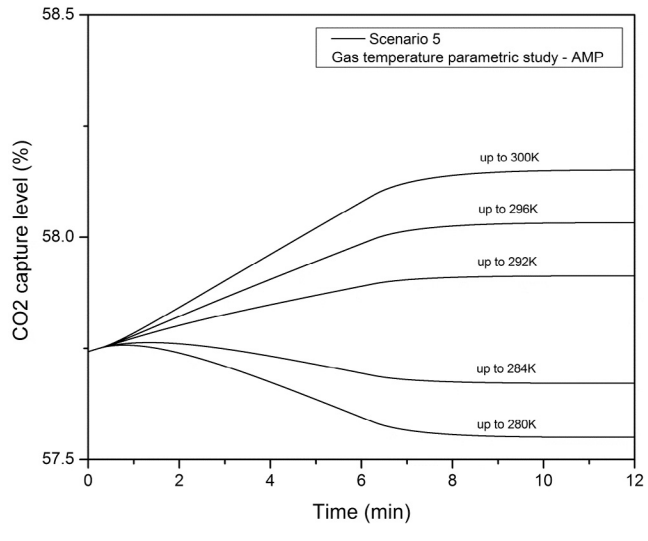

Fig. 10. Gas Temperature parametric study-AMP.

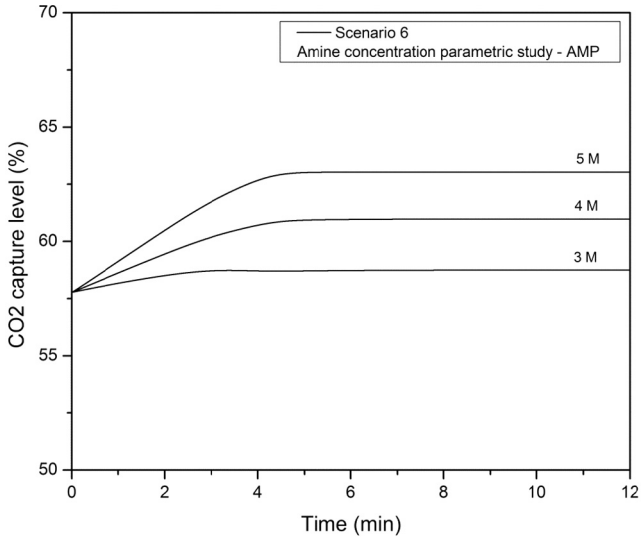

Fig. 11. Inlet amine solvent concentration parametric study-AMP.

flow decreases. The absorption profiles show that the CO_2 capture responds immediately to the gas flow changes and follow almost linear profiles.

5.1.3. Inlet liquid flow parametric study

Fig. 6 shows the effect of the inlet liquid flow linear change on the absorption capacity. For the case that liquid flow increases, the amine capacity is improved raising the capture level. Respectively, less liquid flow causes more difficult absorption lowering the capture level. It is observed that the absorption efficiency has a small response time of two minutes in any disturbances in the liquid flow. As seen in the diagram, initial liquid flow seems to have less impact than gas flow on the final absorption performance as an increase of 20% leads to an improvement of approximately 2% on the CO_2 capture level. Finally, the change is not as linear as in the case of gas flow parametric study.

5.1.4. L/G ratio parametric study

L/G ratio is a characteristic value of an absorption column that is, in certain cases, accurate to conclude over the efficiency of the procedure, due to the existence of an optimum ratio for maximum performance. This section studies the effect of the L/G ratio on the CO_2 capture efficiency. Changes in L/G ratio have been actually studied in the previous sections, as any change in the liquid or gas flow rates leads to respective changes in the L/G ratio. However, in this section linear changes occurring in the gas flow rate are considered, followed by respective linear changes in the liquid flow rate, leading to new constant values of L/G ratio. As mentioned in Table 3, sub-scenario 3a includes the gradual linear change of inlet gas flow rate (up to 10%) and a respective linear increase of the inlet liquid flow rate so as the L/G ratio remains constant in relation to the reference steady state case. As seen in Fig. 7, the absorption level remains almost constant besides the significant change in both gas and liquid flow rates. This confirms the significance of the L/G ratio for the final quantity of CO_2 coming out the column. In case 3b the linear increase of inlet gas flow rate is accompanied by a respective increase of inlet liquid flow rate so as the L/G ratio increases 100% in relation to the reference case ratio. The inlet liquid flow is considered to change in a way that the L/G ratio is immediately increased 100% and remains in this value while both L and G are still increasing. As expected, the absorption performance is improved remarkably, due to the increase of liquid quantity in relation to gas. Following the same pattern, when the gas flow is increased and the liquid is decreased, reducing the L/G ratio 50% the absorption level is decreased. For these two cases, the change in the liquid–gas relation is assumed to occur immediately and as seen in Fig. 7, there is a response interval (3 min) where the absorption performance changes significantly and then is stabilized.

Other two sub-scenarios where tested where the change in the L, G values is instant, not linear as in the previous cases. In Fig. 8, a one-step change in inlet liquid flow was assumed, leading to a new L/G ratio value. As seen in the diagram, a sudden increase in the liquid flow leads to the increase of the CO_2 capture level as expected. A time of approximately 2 min is needed to reach a new steady state condition. On the other hand, when the liquid flow is decreased instantly this time of reaction is approximately 4 min. During these changes the gas flow is assumed to be constant.

5.1.5. Inlet liquid temperature parametric study

This section investigates the effect of inlet liquid temperature on the CO_2 capture level. The inlet liquid temperature is assumed to change linearly up/down to various values during a time interval of 6 min. Then an interval of steady state operation follows. Fig. 9 shows that the absorption performance is considerably influenced by the inlet liquid temperature. Higher temperatures lead to higher absorption level. This correlation seems to be convenient and easily applicable as a solution to enhance the process. However this gain should be examined along with the available solutions for raising the solution temperature and the energy cost for this process. The liquid temperature enters into various correlations leading to the final determination of the overall mass-transfer coefficient playing dramatic role to the final absorption performance. Finally, it is worth mentioning that the absorption efficiency continues to be influenced after the establishment of the new steady state temperatures (after minute 6) and is not yet stabilized after 12 min.

5.1.6. Inlet gas temperature parametric study

In contrast to liquid temperature, inlet gas temperature seems to have trivial effect on the system's absorbing performance. As presented in Fig. 10, even a considerable change in inlet gas temperature (from 288 K to 300 K), leads to a very slight improvement, less than 1% to the overall CO_2 absorption.

5.1.7. Inlet amine solvent concentration parametric study

The final parameter studied is the amine concentration in the lean solution entering the column. As expected, higher amine concentrations raise efficiency, due to increased amine molecules to capture CO_2. However, the effect of the molarity increase is not analogous to this gain. This observation is justified by the fact that the acid-gas vapor pressure is higher over solutions of increased molarity at equivalent acid-gas/amine mole ratio [16]. Increasing the concentration from 2 $kmol/m^3$ to 5 $kmol/m^3$ (150% increase), enhances the removal efficiency from 57% to only 63%.

5.1.8. Sensitivity analysis for AMP solvent

A sensitivity analysis (SA) was performed to determine the effect of the parameters mentioned in the previous sections (independent variables) on CO_2 capture level (dependent variable). The results of this regression analysis will quantify the influence of each parameter on the system performance. The independent variables involved in the analysis are expressed in different units, thus the relative values of the regression coefficients (RC) are not indicative of the actual impact of each parameter. In order to determine this importance, the calculation of Standardized Regression Coefficients (SRC) or beta coefficients is necessary [17]. SRC were calculated by multiplying the RC of each independent variable by its standard deviation and then divide it by the standard deviation of the dependent variable. The new set of regression coefficients indicated the sensitivity of the dependent variable to each independent parameter. The larger coefficient points out the independent variable with the greater influence on the considered dependent variable, while the sign of the coefficient shows whether the increase of the independent variable leads to increase or decrease of the

Table 4
CO_2 removal efficiency (%) statistic results involving inlet liquid and gas flow rates and temperatures, and initial amine solution molarity – AMP.

CO_2 removal efficiency (%)					
Multiple R	0.995				
R^2	0.990				
Adjusted R^2	0.988				
Standard error	0.292				
Observations	25				
	Regression Coefficients	Standardized Regression Coefficients	Standard error	t-Stat	P-Value
Intercept	8.809		7.108	1.240	0.230
Inlet gas flow rate	−12244.1	−0.8318	330.35	−37.07	3.47E−19
Inlet liquid flow rate	463600.4	0.2336	44541.06	10.41	2.75E−09
Inlet liquid temperature	0.2151	0.2857	0.0169	12.72	9.68E−11
Inlet gas temperature	0.0299	0.0396	0.0169	1.764	0.094
Molarity	0.0016	0.4253	8.252E−05	18.91	8.80E−14

Table 5
Regression equation for the dependent variable -AMP, $^{*}\eta\%$: removal percentage.

$Y = a + b^{*} G_{in} + c^{*} L_{in} + d^{*} T_{L,in} + f^{*} C_0$					
Y	a	b	c	d	e
η%	8.809	−12244.1	463600.4	0.2151	0.0016

dependent variable.

The output of this process is presented in Table 4 including RC and SRC values for the dependent variable. As seen in Table 4, the inlet gas flow rate is the most important factor being inversely proportional to the CO_2 capture efficiency. This is also confirmed by previous work in steady state calculations and other literature sources. Inlet liquid temperature and flow rate and amine molarity are also highly affecting proportionally the absorption process performance. It is confirmed that the inlet gas temperature has negligible influence and it will be exempted by the regression equation for the absorption efficiency shown in Table 5.

5.2. MEA dynamic simulations

In order to observe differences between solvents the same approach for MEA was followed as with AMP. For MEA, similar scenarios were simulated, using the conditions of T15 run test conducted by Tontiwachwuthikul described in Table 1. Tables 6 and 7 show the exact scenarios tested for MEA. As before, changes occurring linearly with a duration of 6 min and are followed by a new steady state operation of additional 6 min, while scenarios 3 d,e,f and 6 are considered to happen instantly.

5.2.1. Start-up – MEA

A similar behavior with AMP is observed as the CO_2 capture levels begins to drop after 3 min of operation, reaching approximately 94% (Fig. 12). In Fig. 13, the outlet liquid temperature profiles are presented along the column height. As described in Section 5.1.1, the temperature of the rich solution increases during start-up procedure and the temperature bulge moves higher in the column. In this case, liquid temperature reaches higher values as the heat of reaction between MEA and CO_2 is higher in comparison to AMP for this range of temperatures. In addition, as seen in Fig. 13, the temperature bulge is placed closer to the bottom and its location range is near this area.

Fig. 14 illustrates the rich loading during start-up process. As for AMP, there is a response time of approximately 3 min until rich loading reaches a new steady state value. This delay is also observed in Fig. 12 where the efficiency is still slightly decreasing for 3 min after the gas flow have reached its full load (See Fig. 15).

5.2.2. Inlet gas flow parametric study – MEA

Remarks from this parametric study are similar as with AMP. There are almost linear profiles of overall efficiency and there is an immediate response of the performance to any changes in the initial gas flow entering the column. The impact of such changes is considerable as a change of 20% leads to a 5% decrease of the absorption performance. In addition, the impact appears to be higher for lower values of gas flow.

Table 6
Start-up scenario for MEA – T15.

Start-up	Duration (min)	Inlet gas flow (m^3/sec)	Inlet liquid flow (m^3/sec)
	6	0–0.0028 (linearly increased)	0.0000294 (constant)

Table 7
Dynamic simulation scenarios for MEA – T15.

Phase I: Disturbance scenarios							
1		2		3	4	5	6
Gas flow parametric (m^3/sec)		Liquid flow parametric (m^3/sec)		L/G ratio parametric	Inlet liquid temperature parametric (K)	Inlet gas temperature parametric (K)	Amine initial concentration (mol/m^3)
G	L	G	L	L/G	TL (linearly up/down to)	TG (linearly up/down to)	C_{amine}
From 0.0028 to ± 10, 20% (linearly)	0.0000294 (constant)	0.0028 (constant)	From 0.0000294 to ± 10, 20% (linearly)	a 0.0105 (same as the steady state)	282	282	3000
				b 0.0210	286	286	4000
				c 0.0053	294	294	5000
				d 0.0210 (G constant)	298	298	
				e 0.0053 (G constant)	302	302	
Phase II: New steady state operation (Duration: 6 min) *Operating with the final conditions after the end of the disturbance*							

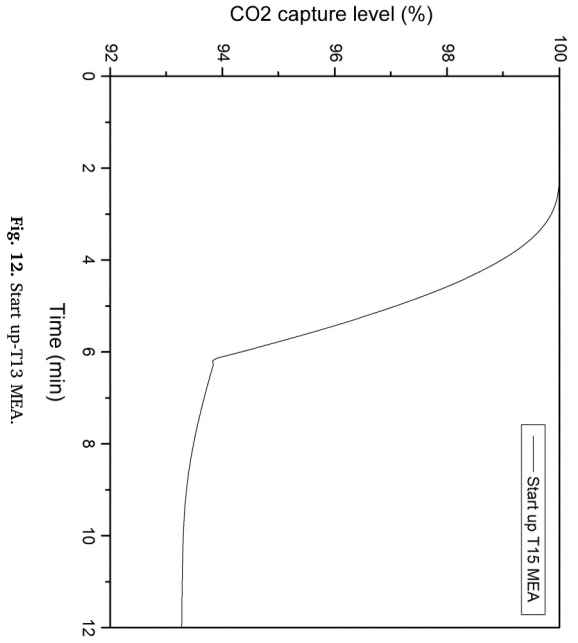

Fig. 12. Start up-T13 MEA.

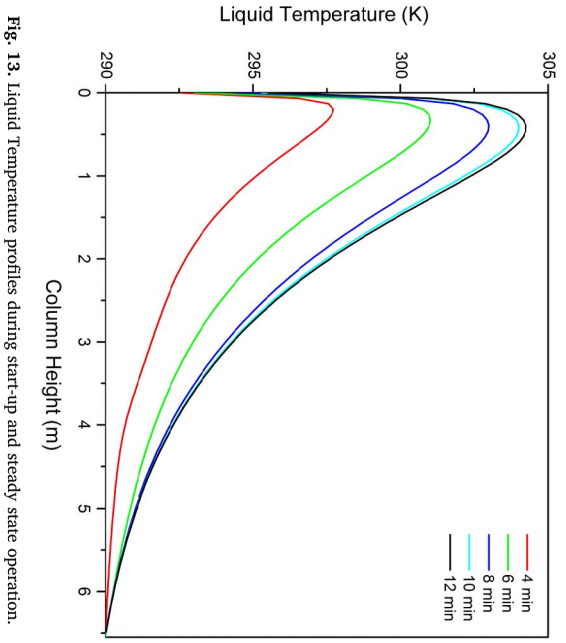

Fig. 13. Liquid Temperature profiles during start-up and steady state operation.

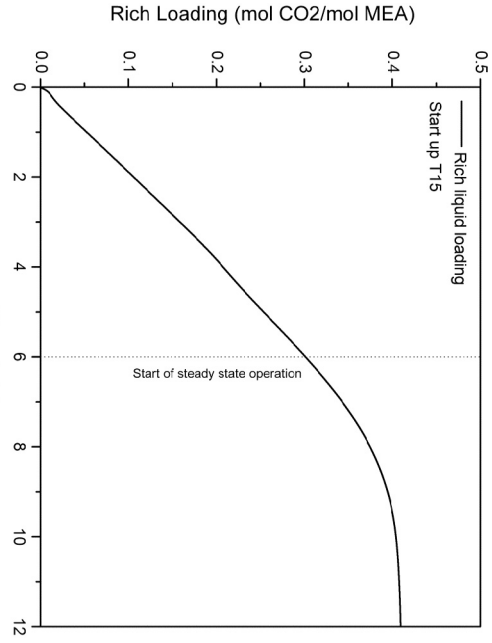

Fig. 14. Rich loading profile for start-up (T15-MEA).

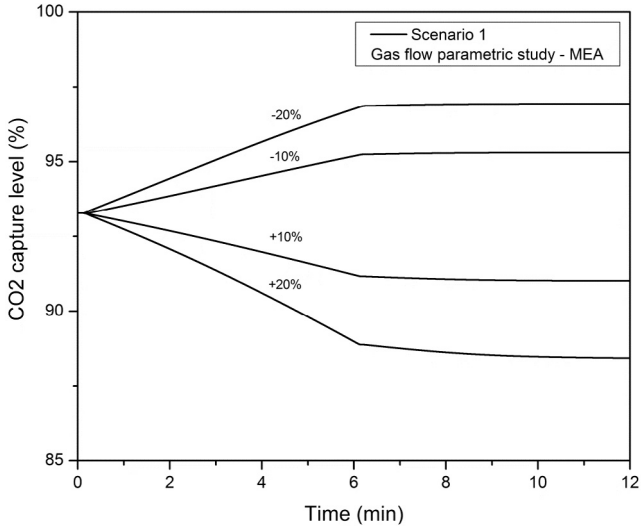

Fig. 15. Gas flow parametric study-MEA.

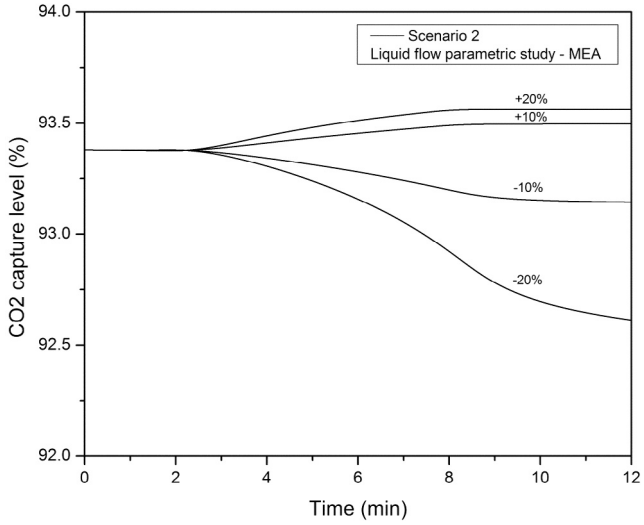

Fig. 16. Liquid flow parametric study-MEA.

5.2.3. Inlet liquid flow parametric study – MEA

As already observed in AMP analysis, the inlet liquid flow has less influence on the overall absorption than inlet gas flow. At the same time, this impact seems to be negligible for higher values of liquid flow as seen in Fig. 16. This is probably due to the fact that the maximum capacity of MEA for the conditions tested is near these values (93–94%) and cannot be significantly further enhanced.

5.2.4. L/G ratio parametric study – MEA

The same scenarios tested in Section 5.1.4 were simulated for MEA solvent under the conditions given in Table 1. Scenario 3a represents a disturbance where both liquid and gas inlet flow rates are gradually increased 10%, keeping the L/G ratio constant through this time, equal to the previous steady state condition. As seen in Fig. 17, the CO_2 absorption performance is slightly lower. This negligible decrease is due to the fact that gas flow has strong impact and its increase hinders absorption, despite the respective increase in liquid flow. For the same reason scenario 3b seems to lead to even lower performance even though L/G ratio is increased 100%. This paradox observation is more intense for this level of absorption, because as mentioned before the phenomenon cannot be further enhanced for this case. Thus, the increase of the gas flow seems to outweigh and hinder absorption. Finally, for scenario 3c the increase of gas flow followed by a respective decrease of liquid flow (L/G ratio reduced 50%) leads to a dramatic drop of CO_2 capture level.

In Fig. 18, two scenarios are presented where there was an instant change of the inlet liquid flow, with constant gas flow, leading to a new L/G ratio (100% higher and 50% lower respectively). As expected from the discussion of the previous paragraph, the enhancement of the procedure is not significant when the L/G ratio is double in relation with steady state, while when the L/G ratio is reduced 50% the difference is considerable. It is notable that Scenarios 3c and 3e refer both in an L/G ratio reduced 50% in relation to the reference steady state case. However, they lead to completely different absorption levels. In 3c, G is increased while L is decreased leading to a very low absorption level (63%), while in 3e only L is changed altering the overall ratio decreasing the absorption level to 87%. This comment confirms the strong impact of inlet gas flow on the overall performance of the process.

5.2.5. Inlet liquid temperature parametric study – MEA

As discussed before, the temperature of the lean solution entering the column is a critical parameter for the absorption performance. Fig. 19 shows this relation, showing that higher inlet temperatures lead to higher absorption. The enhancement is lower for high temperatures and absorption levels, as performance reaches a maximum level.

5.2.6. Inlet gas temperature parametric study

In Fig. 20 the CO_2 capture level range is only 0.5%. This shows the trivial influence of the gas temperature on the absorption process. This observation is also confirmed in the sensitivity analysis following in Section 5.2.8.

5.2.7. Inlet amine solvent concentration parametric study

The amine concentration is obviously a critical factor determining the absorption performance (Fig. 21). The remarks are the same as in the AMP analysis section, showing though once again that the absorption reaches a maximum level and cannot be significantly enhanced beyond this level. Concluding, each factor has specific impact on the absorption, however this impact is not so significant when reaching a maximum performance.

5.2.8. Sensitivity analysis for MEA solvent

The same procedure described in Section 5.1.8 was followed also for MEA case. The results of the sensitivity analysis are presented in Table 8. In this case, the inlet liquid temperature is the dominant parameter influencing the absorption efficiency followed by the inlet

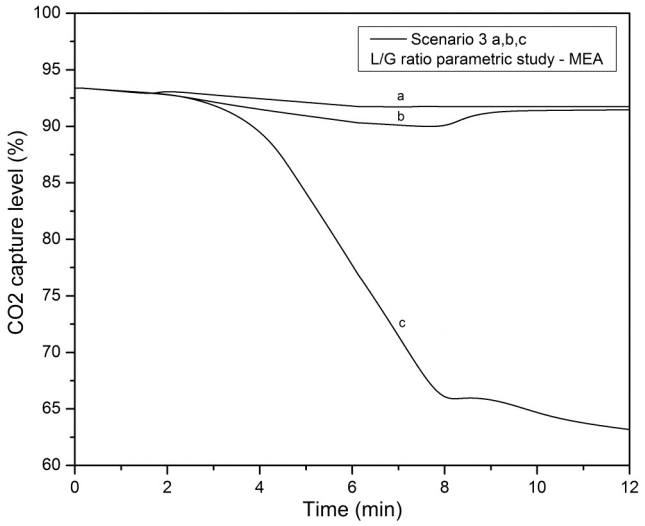

Fig. 17. Scenarios 3 a, b, c: L/G ratio parametric study-MEA.

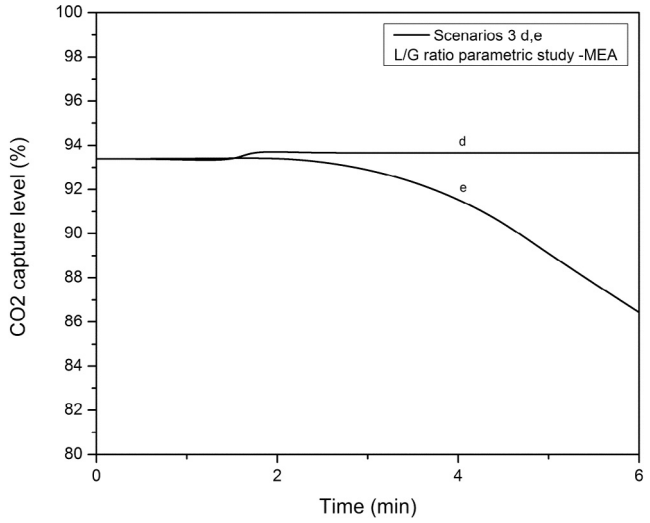

Fig. 18. Scenarios 3 d, e: L/G ratio parametric study-MEA.

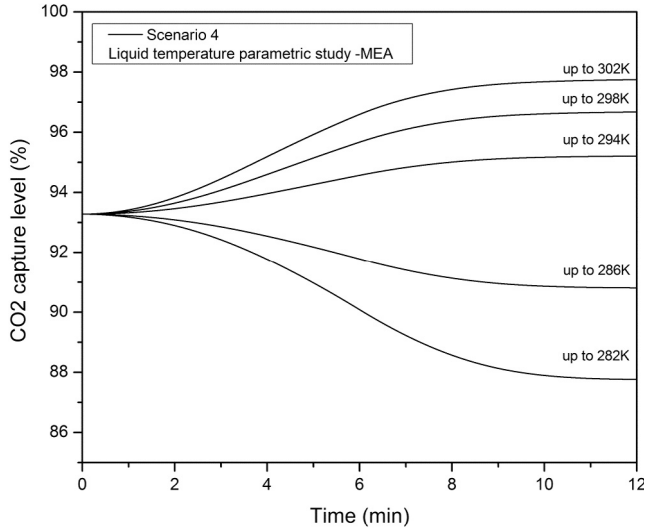

Fig. 19. Liquid Temperature parametric study-MEA.

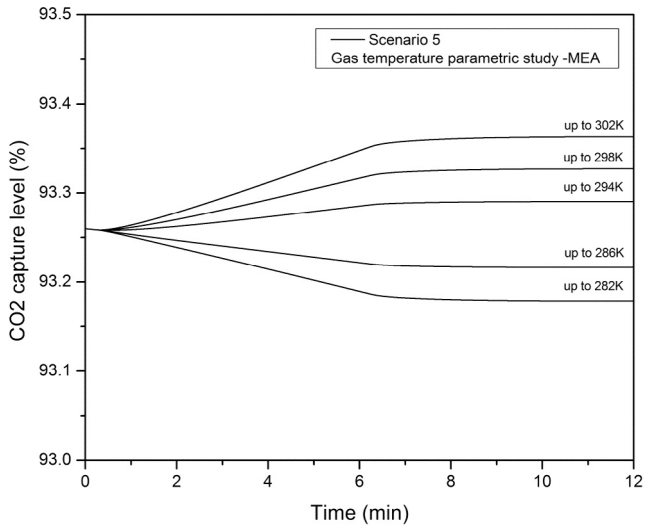

Fig. 20. Gas Temperature parametric study-MEA.

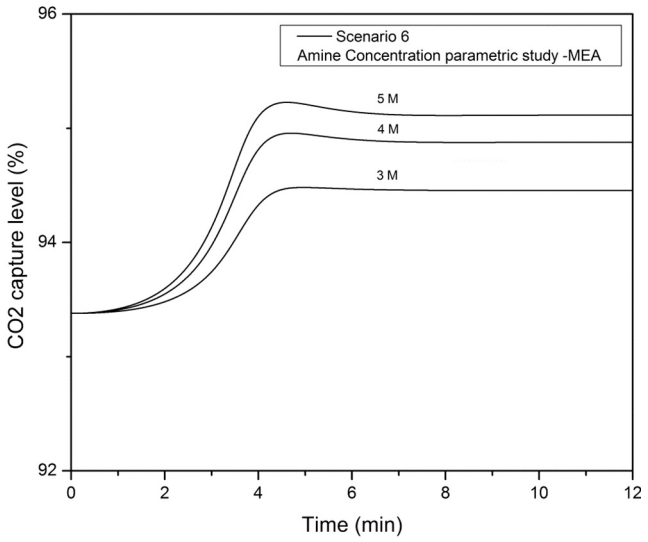

Fig. 21. Inlet amine solvent concentration parametric study-MEA.

gas flow rate. The inlet liquid flow rate and the inlet gas temperature are not statistically important when studying absorption. Table 9 shows the linear correlation deriving from the regression analysis, connecting the independent and the dependent variables.

6. Conclusions

This paper presented a rate-based dynamic model simulating the process of CO_2 reactive absorption by alkanolamines. A set of partial differential equations was presented, deriving from energy and mass balances between gas and liquid bulk phases applying the two-film mass transfer theory. Physical properties for the two phases are extracted from literature. The model simulates a packed absorption column for two dimensions; spatial (axial) and time. The validation of the steady state simulation has been performed in previous work of the researchers. The alkanolamines studied are Monoethanolamine (MEA) and 2-Amino-2-methyl-1-propanol (AMP) which are common and widely used amines.

Mathematical solution in the problem was reached through a built-in code in Matlab®, applying the Finite Differences Method. Various disturbances scenarios as well as the start-up process were simulated in order to draw conclusions on the transient behavior of the system. The independent parameters tested were namely the inlet gas and liquid flow rates, the inlet gas and liquid temperatures, the L/G ratio and the initial amine molarity in the solution. The effect of these factors on the CO_2 final capture level was observed.

The extracted diagrams show some tendencies which are also confirmed by the sensitivity analysis where multiple regression method was performed, considering CO_2 capture level as the dependent variable. Summarizing results, the inlet gas flow is the most critical factor affecting the overall performance of the system, meaning the quantity of CO_2 captured at the top of the column. Increased gas flows hinder the absorption as there is more CO_2 to be captured. The inlet liquid flow impact is not as strong as that of the inlet gas flow. In terms of transient behavior, the response of the system in gas flow changes is direct, while the system needs approximately 2 min to stabilize after linear changes in liquid flow. Another important parameter is the inlet liquid temperature that seems to enhance absorption when raised. In addition, after any changes in inlet liquid temperature there is some time needed in order to reach a new steady state condition. Molarity is as expected a factor that determines the maximum quantity of CO_2 that can be absorbed, however the enhancement is negligible beyond certain molarity values. Instant changes in molarity are followed by a reaction time of 4–5 min in order to reach new steady state condition. Finally inlet gas

Table 8
CO_2 removal efficiency (%) statistic results involving inlet liquid and gas flow rates and temperatures, and initial amine solution molarity – MEA.

CO_2 removal efficiency (%)					
Multiple R	0.987				
R^2	0.974				
Adjusted R^2	0.968				
Standard error	0.410				
Observations	25				
	Regression Coefficients	Standardized Regression Coefficients	Standard error	t-Stat	P-Value
Intercept	−39.66		10.19	−3.90	0.00098
Inlet gas flow rate	−7431.66	−0.6013	453.6653	−16.38	1.158E−12
Inlet liquid flow rate	76294.09	0.0635	44080.667	1.7308	0.0997
Inlet liquid temperature	0.5037	0.7483	0.0247	20.384	2.254E−14
Inlet gas temperature	0.0101	0.01557	0.0238	0.4236	0.6766
Molarity	0.0007	0.2300	0.00012	6.2592	5.201E−06

Table 9
Regression equation for the dependent variable -MEA, $^{*}\eta\%$: removal percentage.

$Y = a + b^{*} G_{in} + c^{*} L_{in} + d^{*} T_{L,in} + f^{*}C_0$					
Y	a	b	c	d	e
η%	−39.66	−7431.66	76294.09	0.5037	0.0007

temperature has negligible effect on absorption and can be ignored when performing statistical analysis. Using the results of the sensitivity analysis a linear regression correlation connecting these parameters was developed calculating the overall CO_2 capture %.

Finally, tests conducted with MEA were simulated with almost optimal conditions reaching CO_2 absorption of over 94%. It was observed that any changes that would enhance absorption, as found through the sensitivity analysis, have reduced effect in this case. This is expected as the absorption performance cannot be further increased.

References

[1] A. Aboudheir, P. Tontiwachwuthikul, R. Idem, Rigorous model for predicting the behavior of CO2 absorption into AMP in packed-bed absorption columns, Ind. Eng. Chem. Res. 45 (2006) 2553–2557.

[2] N.A. Al-Baghli, S.A. Pruess, V.F. Yesavage, M.S. Selim, A rate-based model for the design of gas absorbers for the removal of CO2 and H2S using aqueous solutions of MEA and DEA, Fluid Phase Equilib. 185 (2001) 31–43.

[3] R. Billet, M. Schultes, Predicting mass transfer in packed columns, Chem. Eng. Technol. 16 (1993) 1–9.

[4] A. Chikukwa, N. Enaasen, H.M. Kvamsdal, M. Hillestad, Dynamic modeling of post-combustion CO2 capture using amines – a review, Energy Procedia 23 (2012) 82–91.

[5] P.V. Danckwerts, Absorption by simultaneous diffusion and chemical reaction, T. Faraday Soc. 46 (1950) 300–304.

[6] W.J. DeCoursey, Enhancement factors for gas absorption with reversible reaction, Chem. Eng. Sci. 37 (10) (1982) 1483–1489.

[7] J. Gabrielsen, M. Michelsen, E. Stenby, G. Kontogeorgis, Modeling of CO2 absorber using an AMP solution, AIChE J. 52 (2006) 3443–3451.

[8] J. Gaspar, A.M. Cormos, Dynamic modeling and absorption capacity assessment of CO2 capture process, Int. J. Greenhouse Gas Control 8 (2012) 45–55.

[9] Global CCS Institute, 2016. The Global Status of CCS. Summary Report.

[10] N. Harun, P.L. Douglas, L. Ricardez-Sandoval, E. Croiset, Dynamic simulation of MEA absorption processes for CO2 capture from fossil fuel power plant, Energy Procedia 4 (2011) 1478–1485.

[11] H. Hikita, S. Asal, H. Ishikawa, M. Honda, The kinetics of reactions of CO2 with MEA, DEA and TEA by a rapid mixing method, Chem. Eng. J. 13 (1977) 7–12.

[12] K.A. Hoff, O. Juliussen, O. Falk-Pedersen, H.F. Svendsen, Modeling and experimental study of carbon dioxide absorption in aqueous alkanolamine solutions using a membrane contactor, Ind. Eng. Chem. Res. 43 (2004) 4908–4921.

[13] (EASAC) European Academies Science Advisory Council, 2013. Carbon Capture and Storage in Europe. EASAC policy report 20.

[14] Eurostat website: http://ec.europa.eu/eurostat.

[15] S.A. Jayarathna, B. Lie, M.C. Melaaen, Amine based CO2 capture plant: dynamic modeling and simulations, Int. J. Greenhouse Gas Control. 14 (2013) 282–290.

[16] L. Kohl, R.B. Nielsen, Gas Purification, 5th ed.. Gulf. Huston. USA, 1997.

[17] I.P. Koronaki, The impact of configuration and orientation of solar thermosyphonic systems on night ventilation and fan energy savings, Energy Build. 57 (2013) 119–131.

[18] I.P. Koronaki, L. Prentza, V.D. Papaefthimiou, Parametric analysis using AMP and MEA as aqueous solvents for CO2 absorption, Appl. Thermal Eng. 110 (2017) 126–135.

[19] H.M. Kvamsdal, G.T. Rochelle, Effects of the temperature bulge in CO2 absorption from flue gas by aqueous monoethanolamine, Ind. Eng. Chem. Res. 47 (3) (2008) 867–875.

[20] H.M. Kvamsdal, J.P. Jakobsen, K.A. Hoff, Dynamic modeling and simulation of a CO2 absorber column for post-combustion CO2 capture, Chem. Eng. Process. 48 (2009) 135–144.

[21] A. Lawal, M. Wang, P. Stephenson, G. Koumpouras, H. Yeung, Dynamic modelling and analysis of post-combustion CO2 chemical absorption process for coal-fired power plants, Fuel 89 (2010) 2791–2801.

[22] P. Mores, N. Scenna, S. Mussati, Post-combustion CO2 capture process: equilibrium stage mathematical model of the chemical absorption of CO2 into mono-ethanolamine (MEA) aqueous solution, Chem. Eng. Res. Des. 89 (2011) (2011) 1587–1599.

[23] A.K. Saha, S.S. Bandyopadhyay, A.K. Biswas, Kinetics of absorption of CO2 into aqueous solutions of 2-amino-2-methyl-1-propanol, Chem. Eng. Sci. 50 (1995) 3587–3598.

[24] S. Singh, E. Croiset, P.L. Douglas, M.A. Douglas, Techno-economic study of CO2 capture from an existing coal-fired power plant: MEA scrubbing vs. O2/CO2 recycle combustion, Energy Convers. Manage. 44 (2003) 3073–3091.

[25] Y. Tan, W. Nookuea, H. Li, E. Thorin, Yan Jinyue, Property impacts on carbon capture and storage (CCS) processes, Energy Convers. Manage. 1180 (1016) 204–222.
[26] M. Thiels, D.S.H. Wong, C.H. Yu, J.L. Kang, S.S. Jang, C.S. Tan, Modelling and design of carbon dioxide absorption in rotating packed bed and packed column, IFAC-PapersOnLine 49–7 (2016) 895–900.
[27] P. Tontiwachwuthikul, A. Meisen, J. Lim, CO2 absorption by NaOH, mono-ethanolamine and 2-amino-2-methyl-1-propanol solutions in a packed column, Chem. Eng. Sci. 47 (2) (1992) 381–390.
[28] M. Wang, A.S. Joel, C. Ramshaw, D. Eimer, N.M. Musa, Process intensification for post-combustion CO2 capture with chemical absorption: a critical review, Appl. Energy 158 (2015) 275–291.
[29] W.G. Whitman, The two-film theory of absorption, Chem. Met. Eng. 29 (1923) 147.
[30] S. Ziaii, G.T. Rochelle, T.F. Edgar, Optimum design and control of amine scrubbing in response to electricity and CO2 prices, Energy Procedia 4 (2011) 1683–1690.